Article

Liquid–Crystalline Janus-Type Fullerodendrimers Displaying Tunable Smectic–Columnar Mesomorphism

Julie Lenoble, Stphane Campidelli, Natacha Maringa, Bertrand Donnio, Daniel Guillon, Natalia Yevlampieva, and Robert Deschenaux

J. Am. Chem. Soc., **2007**, 129 (32), 9941-9952• DOI: 10.1021/ja071012o • Publication Date (Web): 20 July 2007

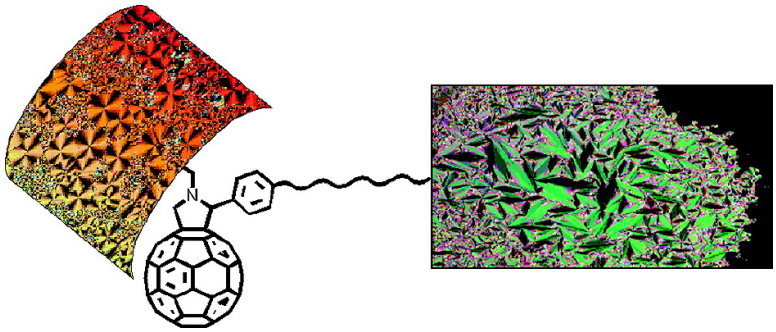

J|A|C|S
ARTICLES
Published on Web 07/20/2007

Liquid−Crystalline Janus-Type Fullerodendrimers Displaying Tunable Smectic−Columnar Mesomorphism

Julie Lenoble,[†] Stéphane Campidelli,[†,⊥] Natacha Maringa,[†] Bertrand Donnio,[‡] Daniel Guillon,*[,‡] Natalia Yevlampieva,*[,§] and Robert Deschenaux*[,†]

Contribution from the Institut de Chimie, Université de Neuchâtel, Avenue de Bellevaux 51, Case Postale 158, 2009 Neuchâtel, Switzerland, Institut de Physique et Chimie des Matériaux de Strasbourg, UMR 7504 (CNRS − Université Louis Pasteur), Groupe des Matériaux Organiques, 23 Rue du Loess, BP 43, 67034 Strasbourg Cedex 2, France, and Institute of Physics, Saint Petersburg State University, Ulianovskaja Street 1, 198504 St. Petersburg, Russia

Received February 12, 2007; E-mail: daniel.guillon@ipcms.u-strasbg.fr; yevlam@paloma.spbu.ru; robert.deschenaux@unine.ch

Abstract: Janus-type liquid−crystalline fullerodendrimers were synthesized via the 1,3-dipolar cycloaddtition of two mesomorphic dendrons and C_{60}. By assembling poly(aryl ester) dendrons functionalized with cyanobiphenyl groups, displaying lamellar mesomorphism, with poly(benzyl ether) dendrons carrying alkyl chains, which display columnar mesomorphism, we could tailor *by design* the liquid−crystalline properties of the title compounds as a function of each dendron size. The liquid−crystalline properties were examined by polarized optical microscopy, differential scanning calorimetry, and X-ray diffraction. Depending on the dendrimer generations, smectic (SmC and/or SmA phases) or columnar (Col_r-*c*2*mm* or Col_r-*p*2*gg* phases) mesomorphism was obtained. The supramolecular organization is governed by (1) the adequacy of the cross-sectional area of the dendrons, (2) the microsegregation of the dendrimer, (3) the deformation of the dendritic core, and (4) the dipolar interactions between the cyanobiphenyl groups. Comparison of the mesomorphic properties of two fullerodendrimers with those of model compounds (fullerene-free analogues) indicated that the C_{60} unit does not influence the type of mesophase that is formed. Molecular properties determined in solution (permanent dipole moment, specific dielectric polarization, molar Kerr constant) confirm that microsegregation persists in solution and strengthen the models proposed for the structure of the mesophases.

Introduction

The successful development of elegant and effective syntheses for the precise functionalization of [60]fullerene (C_{60}), associated with its exceptional photophysical[1] and electrochemical[2] properties, has initiated exciting fields of research in materials science (e.g., photoactive dyads, triads, and polyads, plastic solar cells, organic light emitting diodes).[3]

Organized molecular assemblies are an important class of supramolecular materials. Selective functionalization of C_{60} has enabled the design of Langmuir and Langmuir−Blodgett films,[4] vesicles,[5] self-assembled monolayers,[6] and liquid crystals.[7−12] The search for mesomorphic materials displaying novel properties is a prerequisite for the development of liquid crystal technology by the "bottom-up" approach. Of particular interest are functionalized liquid−crystalline materials which combine the self-organization characteristics of liquid crystals with the properties (redox, magnetic, optical, chiroptical) of the functional entity. In this respect, C_{60} is an excellent unit for the design of photo- and electroactive liquid crystals.

Four approaches have been reported for the design of fullerene-containing thermotropic liquid crystals. First, addition of liquid−crystalline addends[7,8,11] to C_{60} by applying either the Bingel reaction[13] or the 1,3-dipolar cycloaddition reaction[14] produced mesomorphic methanofullerenes or fulleropyrrolidines, respectively. Nematic, chiral nematic, smectic A, smectic B,

[†] Université de Neuchâtel.
[‡] Institut de Physique et Chimie des Matériaux de Strasbourg.
[§] Saint Petersburg State University.
[⊥] Current address: Laboratoire d'Electronique Moléculaire, CEA Saclay, 91191 Gif sur Yvette, France.

(1) (a) Guldi, D. M. *Chem. Commun.* **2000**, 321. (b) Guldi, D. M. *Chem. Soc. Rev.* **2002**, *31*, 22.
(2) Echegoyen, L.; Echegoyen, L. E. *Acc. Chem. Res.* **1998**, *31*, 593.
(3) (a) Nakamura, E.; Isobe, H. *Acc. Chem. Res.* **2003**, *36*, 807. (b) Nierengarten, J.-F. *New J. Chem.* **2004**, *28*, 1177. (c) Segura, J. L.; Martín, N.; Guldi, D. M. *Chem. Soc. Rev.* **2005**, *34*, 31. (d) Hoppe, H.; Sariciftci, N. S. *J. Mater. Chem.* **2006**, *16*, 45. (e) Guldi, D. M.; Rahman, G. M. A.; Sgobba, V.; Ehli, C. *Chem. Soc. Rev.* **2006**, *35*, 471. (f) Martín, N. *Chem. Commun.* **2006**, 2093. (g) Figueira-Duarte, T. M.; Gégout, A.; Nierengarten, J.-F. *Chem. Commun.* **2007**, 109. (h) Yang, X.; Loos, J. *Macromolecules* **2007**, *40*, 1353.
(4) (a) Cardullo, F.; Diederich, F.; Echegoyen, L.; Habicher, T.; Jayaraman, N.; Leblanc, R. M.; Stoddart, J. F.; Wang, S. P. *Langmuir* **1998**, *14*, 1955. (b) Felder, D.; Gallani, J.-L.; Guillon, D.; Heinrich, B.; Nicoud, J.-F.; Nierengarten, J.-F. *Angew. Chem., Int. Ed.* **2000**, *39*, 201. (c) Nierengarten, J.-F.; Eckert, J.-F.; Rio, Y.; del Pilar Carreon, M.; Gallani, J.-L.; Guillon, D. *J. Am. Chem. Soc.* **2001**, *123*, 9743. (d) Burghardt, S.; Hirsch, A.; Medard, N.; Kachfhe, R. A.; Ausseré, D.; Valignat, M.-P.; Gallani, J.-L. *Langmuir* **2005**, *21*, 7540.
(5) Burghardt, S.; Hirsch, A.; Schade, B.; Ludwig, K.; Böttcher, C. *Angew. Chem., Int. Ed.* **2005**, *44*, 2976.
(6) (a) Echegoyen, L.; Echegoyen, L. E. *Acc. Chem. Res.* **1998**, *31*, 593. (b) Bustos, E.; Manríquez, J.; Echegoyen, L.; Godínez, L. A. *Chem. Commun.* **2005**, 1613. (c) Shirai, Y.; Cheng, L.; Chen, B.; Tour, J. M. *J. Am. Chem. Soc.* **2006**, *128*, 13479. (d) Bonifazi, D.; Enger, O.; Diederich, F. *Chem. Soc. Rev.* **2007**, *36*, 390.

and columnar phases were observed. The second approach involves the formation of noncovalent complexes: reaction of a liquid−crystalline cyclotriveratrylene with C_{60} provided a complex that displayed nematic and cubic phases,[12a] while a spin-coated dendritic porphyrin and C_{60} gave a nonidentified columnar phase.[12b] In the third approach, grafting of five rodlike aromatic units around one pentagon of C_{60} provided cone-shaped molecules that showed either columnar[9a] or lamellar[9b] phases. In the fourth approach, a 1:1 mixture of two nonmesomorphic compounds (i.e., a methanofullerene derivative and a disclike molecule) showed the formation of a columnar phase.[10]

The first approach is the most versatile one, owing to the large variety of liquid−crystalline addends that can be grafted onto C_{60}. Furthermore, the use of dendrimers for the design of mesomorphic materials (e.g., dendritic liquid−crystalline methanofullerenes[7a,b] and dendritic liquid−crystalline fulleropyrrolidines)[7f,h] is appealing because specific structural features, such as the generation, the multiplicity of the branches, the connectivity, flexibility, and polarity, can be adjusted to fine-tune the liquid−crystalline behavior.

Glycine and sarcosine (*N*-methyl glycine) have predominantly been used to construct liquid−crystalline fulleropyrrolidines. However, the use of *N*-substituted glycines enabled the introduction of a second addend onto C_{60} leading to liquid−crystalline fullerene−OPV conjugates[7c] and liquid−crystalline fullerene−ferrocene dyads.[7d,g] If the second addend is a mesomorphic dendrimer, liquid−crystalline fullero(codendrimers) or, in other words, liquid−crystalline Janus-type fulleropyrrolidines are obtained.

There are clearly more methods available for the control of the liquid−crystalline properties of codendrimers than of dendrimers. For example, when two different dendrons are assembled, their generation, relative proportions, and location within the molecule can be varied, and each modification can be used, in principle, to control the nature of the mesophases.[15] By exploiting this modular construction of mesomorphic macromolecules, we envisioned that the liquid−crystalline properties of fullero(codendrimers) could be tuned by changing the generation of the dendrons located on C_{60}. This approach represents an attractive way for the design of fullerene-containing liquid crystals with tailor-made mesomorphic properties. Therefore, the assembly via 1,3-dipolar cycloaddition of poly(aryl ester) dendrons functionalized with cyanobiphenyl groups with poly(benzyl ether) dendrons carrying alkyl chains was attempted. These dendrimers were selected with the expectation that their different structural characteristics and properties would influence the overall liquid−crystalline behavior. In such structures, C_{60} is hidden in the organic matrix, and the supramolecular organization should only depend on the dendrons and should not be altered by the presence of the isotropic C_{60} hard sphere. Furthermore, owing to the different nature of the dendrons, microsegregation should be obtained, leading to long-range organization within the liquid crystal state.

We describe, herein, the synthesis, characterization, mesomorphic properties, and supramolecular organization of fullero(codendrimers) **1**−**6** (Charts 1 and 2) and demonstrate the key role played by the association of the selected dendrons on the formation, structure, and nature of the mesophases. Two model compounds, **MC-I** and **MC-II** (Chart 3), which are the fullerene-free analogues of **5** and **1**, respectively, were used to put to the fore a possible influence of C_{60} on the liquid−crystalline behavior and supramolecular organization. Finally, the solution properties (permanent dipole moment, specific dielectric polarization, and molar Kerr constant) of dendrons **13** and **17** and corresponding fulleropyrrolidine **3** were investigated to establish the influence of each dendron on the overall behavior of the title compounds. All the dendrons described herein were synthesized via a convergent approach.[16]

Results and Discussion

Design. This study focuses on the combination of either second (**10**, Scheme 1) or third (**15**, Scheme 2) generation poly(benzyl ether) dendrons with first (**16**, Scheme 3), second (**17**, Scheme 4), or third (**18**, Scheme 5) generation poly(aryl ester) dendrons. Thus, six fullero(codendrimers) were prepared and classified within two series according to their mesomorphic properties, that is, compounds **1**−**3** for the first series (Chart 1, columnar mesomorphism) and compounds **4**−**6** for the second series (Chart 2, smectic mesomorphism).

Synthesis. Preparation of **1**−**6** (Charts 1 and 2) requires the synthesis of the dendritic-type *N*-amino acid derivatives **10** (Scheme 1) and **15** (Scheme 2). Synthesis of **16**−**18** has previously been published,[7f] and compounds **7** and **11** were prepared as described in the literature.[17a]

(7) (a) Dardel, B.; Deschenaux, R.; Even, M.; Serrano, E. *Macromolecules* **1999**, *32*, 5193. (b) Dardel, B.; Guillon, D.; Heinrich, B.; Deschenaux, R. *J. Mater. Chem.* **2001**, *11*, 2814. (c) Campidelli, S.; Deschenaux, R.; Eckert, J.-F.; Guillon, D.; Nierengarten, J.-F. *Chem. Commun.* **2002**, 656. (d) Campidelli, S.; Vázquez, E.; Milic, D.; Prato, M.; Barberá, J.; Guldi, D. M.; Marcaccio, M.; Paolucci, D.; Paolucci, F.; Deschenaux, R. *J. Mater. Chem.* **2004**, *14*, 1266. (e) Allard, E.; Oswald, F.; Donnio, B.; Guillon, D.; Delgado, J. L.; Langa, F.; Deschenaux, R. *Org. Lett.* **2005**, *7*, 383. (f) Campidelli, S.; Lenoble, J.; Barberá, J.; Paolucci, F.; Marcaccio, M.; Paolucci, D.; Deschenaux, R. *Macromolecules* **2005**, *38*, 7915. (g) Campidelli, S.; Pérez, L.; Rodríguez-López, J.; Barberá, J.; Langa, F.; Deschenaux, R. *Tetrahedron* **2006**, *62*, 2115. (h) Lenoble, J.; Maringa, N.; Campidelli, S.; Donnio, B.; Guillon, D.; Deschenaux, R. *Org. Lett.* **2006**, *8*, 1851. (i) Campidelli, S.; Vázquez, E.; Milic, D.; Lenoble, J.; Atienza-Castellanos, C.; Sarova, G.; Guldi, D. M.; Deschenaux, R.; Prato, M. *J. Org. Chem.* **2006**, *71*, 7603. (j) Campidelli, S.; Brandmüller, T.; Hirsch, A.; Saez, I. M.; Goodby, J. W.; Deschenaux, R. *Chem. Commun.* **2006**, 4282. (k) Gottis, S.; Kopp, C.; Allard, E.; Deschenaux, R. *Helv. Chim. Acta* **2007**, *90*, 957. (l) Deschenaux, R.; Donnio, B.; Guillon, D. *New J. Chem.* **2007**, *31*, 1064.

(8) Tirelli, N.; Cardullo, F.; Habicher, T.; Suter, U. W.; Diederich, F. *J. Chem. Soc., Perkin Trans. 2* **2000**, 193.

(9) (a) Sawamura, M.; Kawai, K.; Matsuo, Y.; Kanie, K.; Kato, T.; Nakamura, E. *Nature* **2002**, *419*, 702. (b) Zhong, Y.-W.; Matsuo, Y.; Nakamura, E. *J. Am. Chem. Soc.* **2007**, *129*, 3052.

(10) Bushby, R. J.; Hamley, I. W.; Liu, Q.; Lozman, O. R.; Lydon, J. E. *J. Mater. Chem.* **2005**, *15*, 4429.

(11) (a) Felder-Flesch, D.; Rupnicki, L.; Bourgogne, C.; Donnio, B.; Guillon, D. *J. Mater. Chem.* **2006**, *16*, 304. (b) Mamlouk, H.; Heinrich, B.; Bourgogne, C.; Donnio, B.; Guillon, D.; Felder-Flesch, D. *J. Mater. Chem.* **2007**, *17*, 2199.

(12) (a) Felder, D.; Heinrich, B.; Guillon, D.; Nicoud, J.-F.; Nierengarten, J.-F. *Chem.−Eur. J.* **2000**, *6*, 3501. (b) Kimura, M.; Saito, Y.; Ohta, K.; Hanabusa, K.; Shirai, H.; Kobayashi, N. *J. Am. Chem. Soc.* **2002**, *124*, 5274.

(13) (a) Bingel, C. *Chem. Ber.* **1993**, *126*, 1957. (b) Nierengarten, J.-F.; Herrmann, A.; Tykwinski, R. R.; Rüttimann, M.; Diederich, F.; Boudon, C.; Gisselbrecht, J.-P.; Gross, M. *Helv. Chim. Acta* **1997**, *80*, 293. (c) Camps, X.; Hirsch, A. *J. Chem. Soc., Perkin Trans. 1* **1997**, 1595.

(14) (a) Prato, M.; Maggini, M. *Acc. Chem. Res.* **1998**, *31*, 519. (b) Tagmatarchis, N.; Prato, M. *Synlett* **2003**, 768.

(15) Bury, I.; Heinrich, B.; Bourgogne, C.; Guillon, D.; Donnio, B. *Chem.−Eur. J.* **2006**, *12*, 8396.

(16) (a) Hawker, C. J.; Fréchet, J. M. J. *J. Am. Chem. Soc.* **1990**, *112*, 7638. (b) Grayson, S. M.; Fréchet, J. M. J. *Chem. Rev.* **2001**, *101*, 3819. (c) Fréchet, J. M. J. *J. Polym. Sci., Part A: Polym. Chem.* **2003**, *41*, 3713.

(17) (a) Percec, V.; Cho, W.-D.; Ungar, G.; Yeardley, D. J. P. *J. Am. Chem. Soc.* **2001**, *123*, 1302. (b) Percec, V.; Glodde, M.; Bera, T. K.; Miura, Y.; Shiyanovskaya, I.; Singer, K. D.; Balagurusamy, V. S. K.; Heiney, P. A.; Schnell, I.; Rapp, A.; Spiess, H.-W.; Hudson, S. D.; Duan, H. *Nature* **2002**, *419*, 384. (c) Percec, V.; Mitchell, C. M.; Cho, W.-D.; Uchida, S.; Glodde, M.; Ungar, G.; Zeng, X.; Liu, Y.; Balagurusamy, V. S. K.; Heiney, P. A. *J. Am. Chem. Soc.* **2004**, *126*, 6078. (d) Percec, V.; Dulcey, A. E.; Peterca, M.; Ilies, M.; Sienkowska, M. J.; Heiney, P. A. *J. Am. Chem. Soc.* **2005**, *127*, 17902.

Chart 1

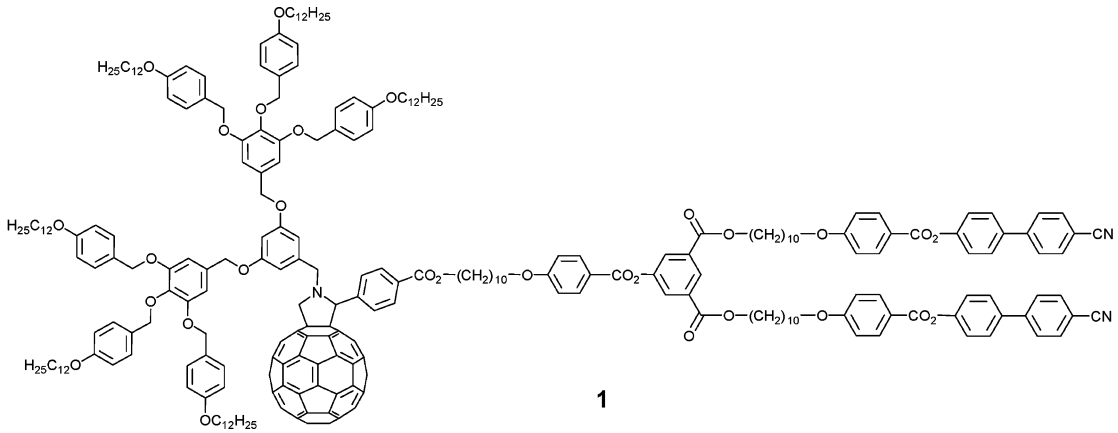

1

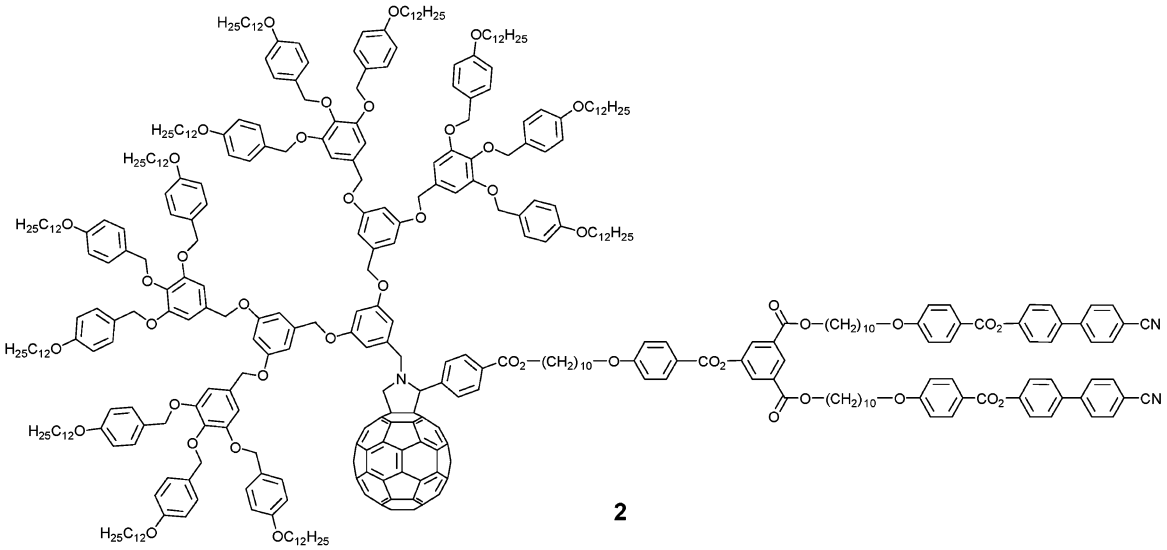

2

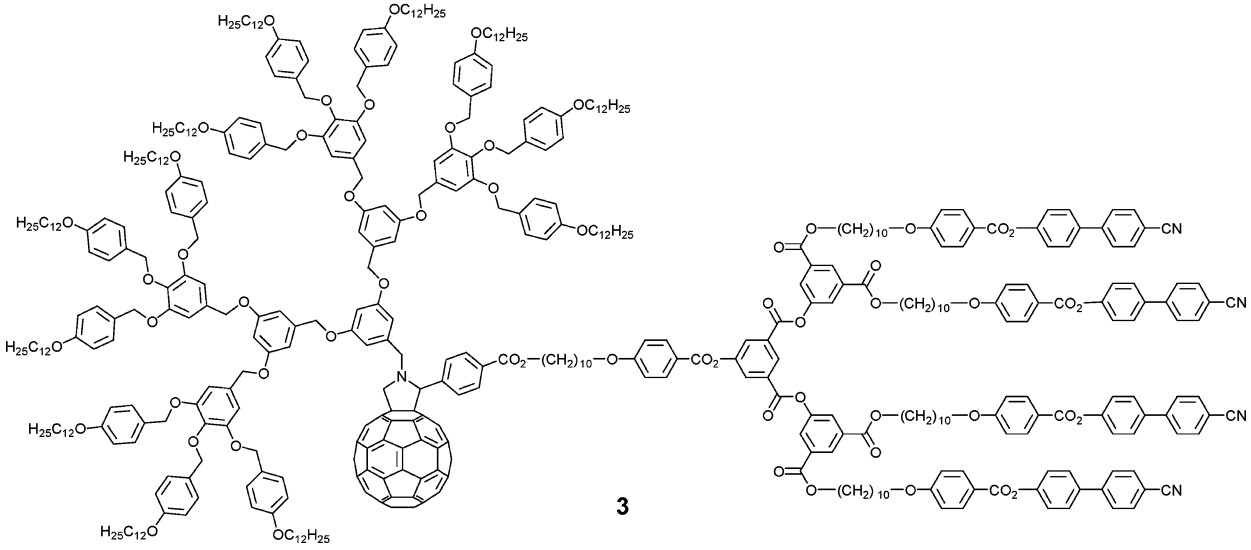

3

Etherification of 3,5-dihydroxybenzaldehyde with **7** led to **8** (Scheme 1). Reductive amination of **8** with glycine methyl ester and $NaBH_3CN$ gave **9**, which was hydrolyzed to furnish second-generation amino acid derivative **10**. The third-generation amino acid derivative **15** was prepared from benzyl alcohol intermediate **11** (Scheme 2). Chlorination of **11** gave **12**, which was reacted with 3,5-dihydroxybenzaldehyde to give aldehyde **13**. Reductive amination of **13** with glycine methyl ester and $NaBH_3CN$ gave **14**, which was hydrolyzed to amino acid derivative **15**.

Addition of **10** and **16** to C_{60} led to **1** (Scheme 3). Fulleropyrrolidines **2**−**6** were prepared analogously from the

Chart 2

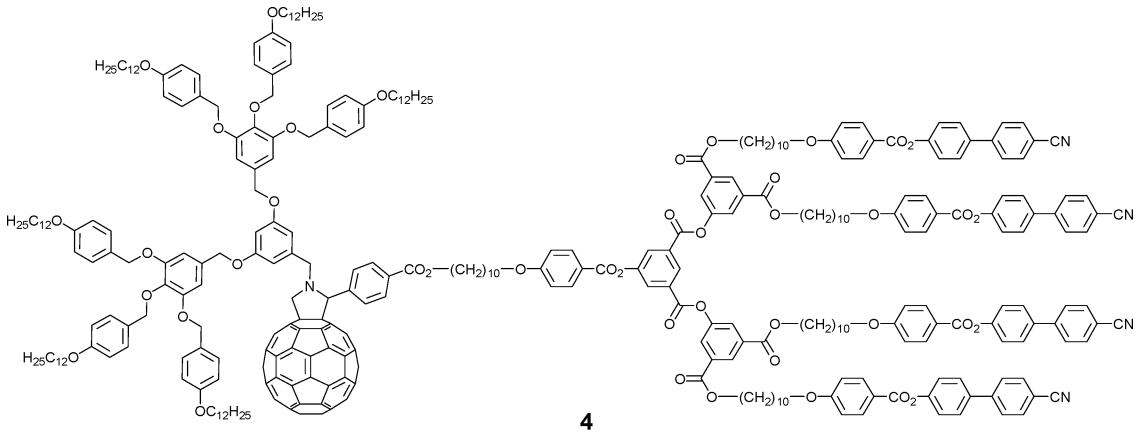

4

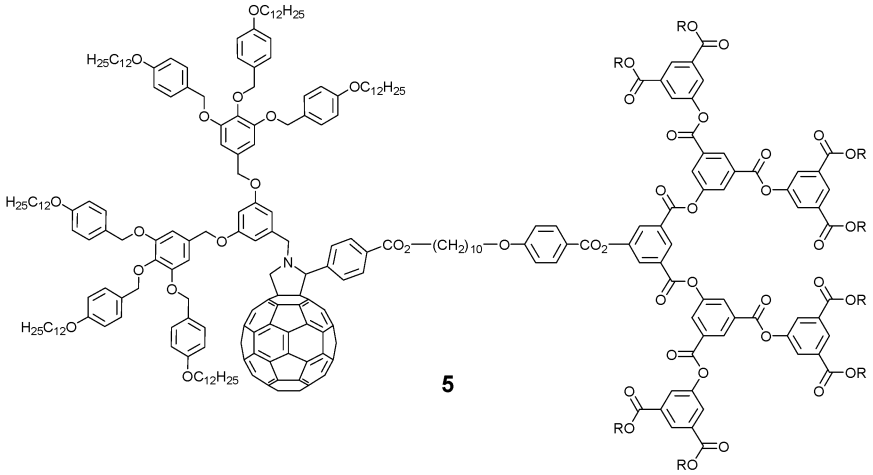

5

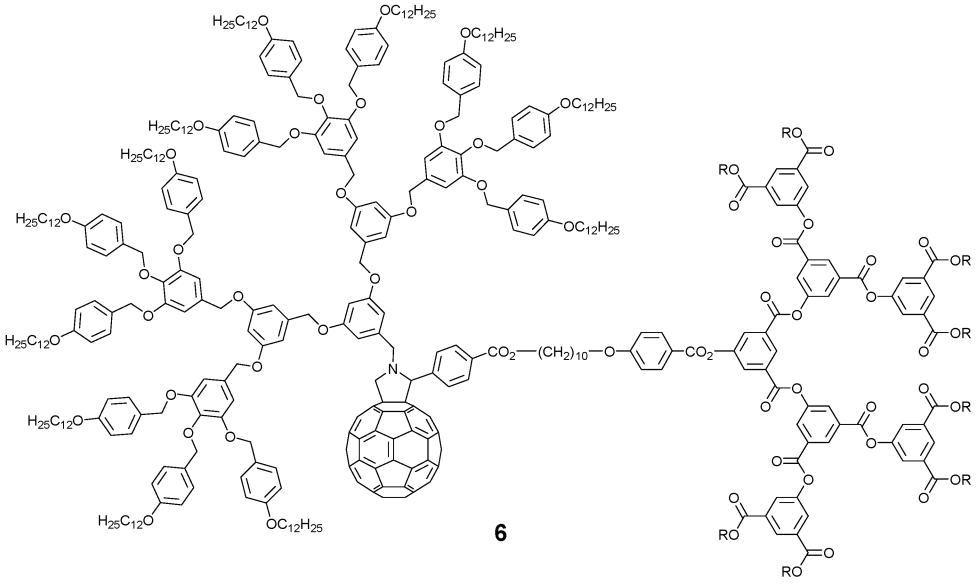

6

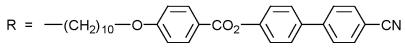

corresponding aldehyde and amino acid dendrons, that is, **15** + **16** → **2** (Scheme 3), **15** + **17** → **3** (Scheme 4), **10** + **17** → **4** (Scheme 4), **10** + **18** → **5** (Scheme 5), and **15** + **18** → **6** (Scheme 5).

Model compounds **MC-I** and **MC-II** were prepared by esterification of second-generation poly(benzyl ether)-CO_2H dendron[17a] with either third- or first-generation poly(aryl ester)-OH dendron,[7f] respectively.

The structure and purity of all compounds were confirmed by ^{1}H NMR spectroscopy, GPC (all compounds were monodisperse), and elemental analysis. The UV−vis spectra of **1**−**6** are in agreement with the fulleropyrrolidine structure.[1]

Chart 3

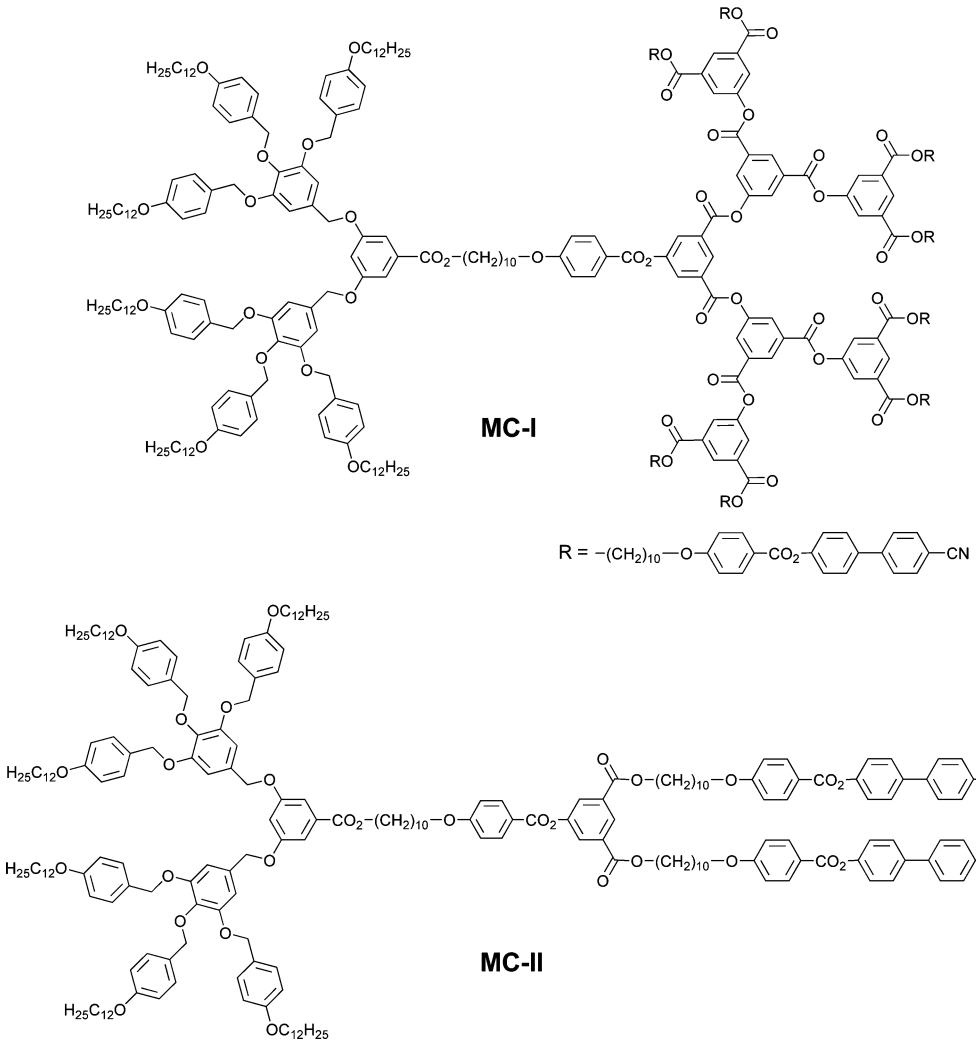

Liquid−Crystalline Properties. The mesomorphic and thermal properties of the poly(benzyl ether) aldehydes **8** and **13**, *N*-substituted gylcine methyl esters **9** and **14**, fulleropyrrolidines **1**−**6**, and model compounds **MC-I** and **MC-II** were investigated by polarized optical microscopy (POM) and differential scanning calorimetry (DSC). The phase transition temperatures and enthalpies are reported in Table 1. The mesophases displayed by **1**−**6**, **MC-I**, and **MC-II** were characterized by X-ray diffraction (XRD). The properties of aldehyde derivatives **16**−**18** have previously been reported, all demonstrating a smectic A phase.[7f] The liquid−crystalline behavior of **10** and **15** was not investigated as the products were only purified by precipitation.

The aldehyde derivatives (**8** and **13**) and *N*-substituted glycine methyl ester derivatives (**9** and **14**) formed columnar phases. The latter were identified by POM from the formation of pseudo-focal conic textures (Figures S1−S4). Compound **9** gave an additional cubic phase, identified by the formation of a viscous, isotropic fluid. Thus, **8**, **9**, **13**, and **14** showed liquid−crystalline behavior typical of poly(benzyl ether) dendrimers.[17]

From the point of view of their liquid−crystalline properties, **1**−**6** can be classified within two families: compounds **1**−**3**, which gave rise to columnar phases, and compounds **4**−**6**, which showed smectic phases. Centered (*c*2*mm*) (**1** and **3**) or noncentered (*p*2*gg*) (**2**) rectangular columnar phases were obtained for **1**−**3**, and smectic A (**5** and **6**) or smectic A and smectic C (**4**) phases were observed for **4**−**6**. The columnar (pseudo-focal conic texture), smectic A (focal conic and homeotropic textures), and smectic C (focal conic and Schlieren textures) phases were identified by POM (Figures S5−S7). As an illustrative example, the DSC thermogram of **2** is shown in Figure S8.

Comparison of the isotropization temperatures emphasized the influence of the poly(aryl ester) dendrons on the thermal stability of the liquid−crystalline phases. Compounds **5** and **6**, with third-generation poly(aryl ester) dendron, showed the highest isotropization temperatures (210 °C for **5** and 209 °C for **6**); in contrast, the size of the poly(benzyl ether) dendron (second generation for **5** and third generation for **6**) had no influence on the isotropization temperature. Decreasing the poly(aryl ester) dendron generation resulted in a decrease in clearing point [155 °C for **4**, and 152 °C for **3**, both second-generation poly(aryl ester) dendron], independent of the observed mesophase. Finally, the clearing point of **1** and **2** confirmed that the poly(benzyl ether) dendron had no influence on the isotropization temperature (105 °C for **1** and 109 °C for **2**).

The isotropic-to-isotropic liquid transition observed for **1** was detected by DSC. No change in texture was observed by POM. Identification of this transition was made by XRD (see below). It is possible that some interactions between molecules persist through the first isotropic state resulting in some locally

Scheme 1 [a]

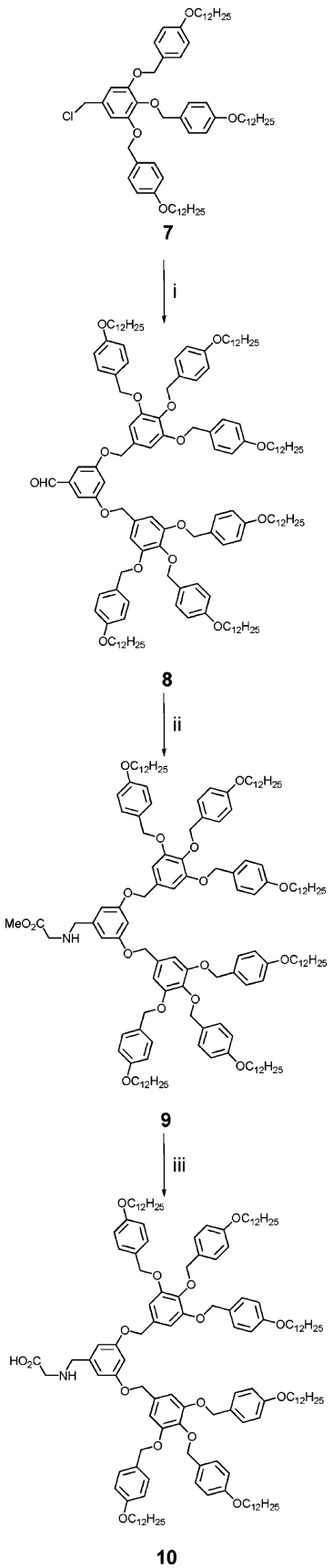

[a] (i) 3,5-Dihydroxybenzaldehyde, K_2CO_3, DMF/THF, 70 °C, overnight, 82%; (ii) glycine methyl ester hydrochloride, Et_3N, THF/MeOH, room temperature (rt), 1 h, then $NaBH_3CN$, overnight, 70%; (iii) NaOH 4 N, THF/MeOH, rt, 1 h, then HCl (2 N), 98%.

organized large aggregates, which are no longer present after the second transition.[18]

The liquid−crystalline properties of **1**−**6** are dependent on the respective generation of each dendron. When the generation of the poly(benzyl ether) dendron is higher than that of the poly(aryl ester) dendron, columnar mesomorphism is observed (i.e., for **1**−**3**); conversely, when the generation of the poly(aryl ester) dendron is higher (i.e., for **5**) than or the same as (i.e., for **4** and **6**) that of the poly(benzyl ether), smectic mesomorphism is observed. The liquid−crystalline properties of **1**−**6** can thus be tuned by design.

Supramolecular Organization. Smectic Phases. The X-ray diffraction patterns of **4**−**6** are characterized by a series of four to six sharp signals in the small angle region in the 1:2:3:4:5:6 ratio and a diffuse halo in the wide-angle region at about 4.5 Å. These features are characteristic of smectic phases. The observation of a large number of diffraction peaks is an indication that the piling of the smectic layers is very well developed and suggests an effective microsegregation (Table 2 and Figure S9).

From room temperature up to 50 °C, the X-ray patterns of **4** are typical of an amorphous phase. They exhibit small- and wide-angle diffuse signals, indicative of a short-range order structuring. Above this temperature, **4** self-organizes into smectic A and smectic C phases. The layer spacing of **4** is almost constant (d = 121.5 Å at 75 °C down to 117.4 Å at 150 °C) within the temperature range of the mesomorphic domain (Table S1), despite the smectic C-to-smectic A phase transformation observed by POM. This behavior indicates that within the smectic A phase, there is a randomly oriented tilt of the mesogenic groups with a tilt value similar to that found in the smectic C phase.[19]

Compound **5** exhibits a lamellar structure from about 70 °C up to the isotropization temperature (210 °C). Interestingly, increasing temperature induces a sharpening of the small-angle diffraction peaks, indicating that the lamellar stacking extends over larger and larger correlation distances. In addition, the lamellar spacing decreases smoothly from 128.6 Å (75 °C) to 121.4 Å (200 °C) (Table S1), in agreement with the temperature variation of lamellar spacing in a smectic A phase. Below 70 °C, **5** exists in an amorphous (glassy) state characterized by broad small- and wide-angle signals showing the existence of a poorly developed lamellar ordering.

The X-ray diffraction patterns of **6**, up to 140 °C, show a disordered structure (broad and weak equidistant diffraction signals in the small-angle region and a diffuse halo at 4.5 Å in the wide-angle region). Such patterns correspond to amorphous organizations with a low lamellar ordering extending only over short distances. Above 140 °C, X-ray diffraction patterns show the presence of a smectic structure. The X-ray patterns remain unchanged up to 200 °C (Table S1).

From the above results, two important observations can be made. Despite the high molecular weight of the materials (5.5

(18) (a) Goodby, J. W.; Waugh, M. A.; Stein, S. M.; Chin, E.; Pindak, R.; Patel, J. S. *J. Am. Chem. Soc.* **1989**, *111*, 8119. (b) Goodby, J. W.; Dunmur, D. A.; Collings, P. J. *Liq. Cryst.* **1995**, *19*, 703. (c) Kutsumizu, S.; Kato, R.; Yamada, M.; Yano, S. *J. Phys. Chem. B* **1997**, *101*, 10666. (d) Kutsumizu, S.; Yamaguchi, T.; Kato, R.; Yano, S. *Liq. Cryst.* **1999**, *26*, 567. (e) Nashiyama, I.; Yamamoto, J.; Goodby, J. W.; Yokoyama, H. *J. Mater. Chem.* **2001**, *11*, 2690.
(19) (a) de Vries, A.; Ekachai, A.; Spielberg, N. *Mol. Cryst. Liq. Cryst.* **1979**, *49*, 143. (b) de Vries, A. *J. Chem. Phys.* **1979**, *71*, 25.

Scheme 2 [a]

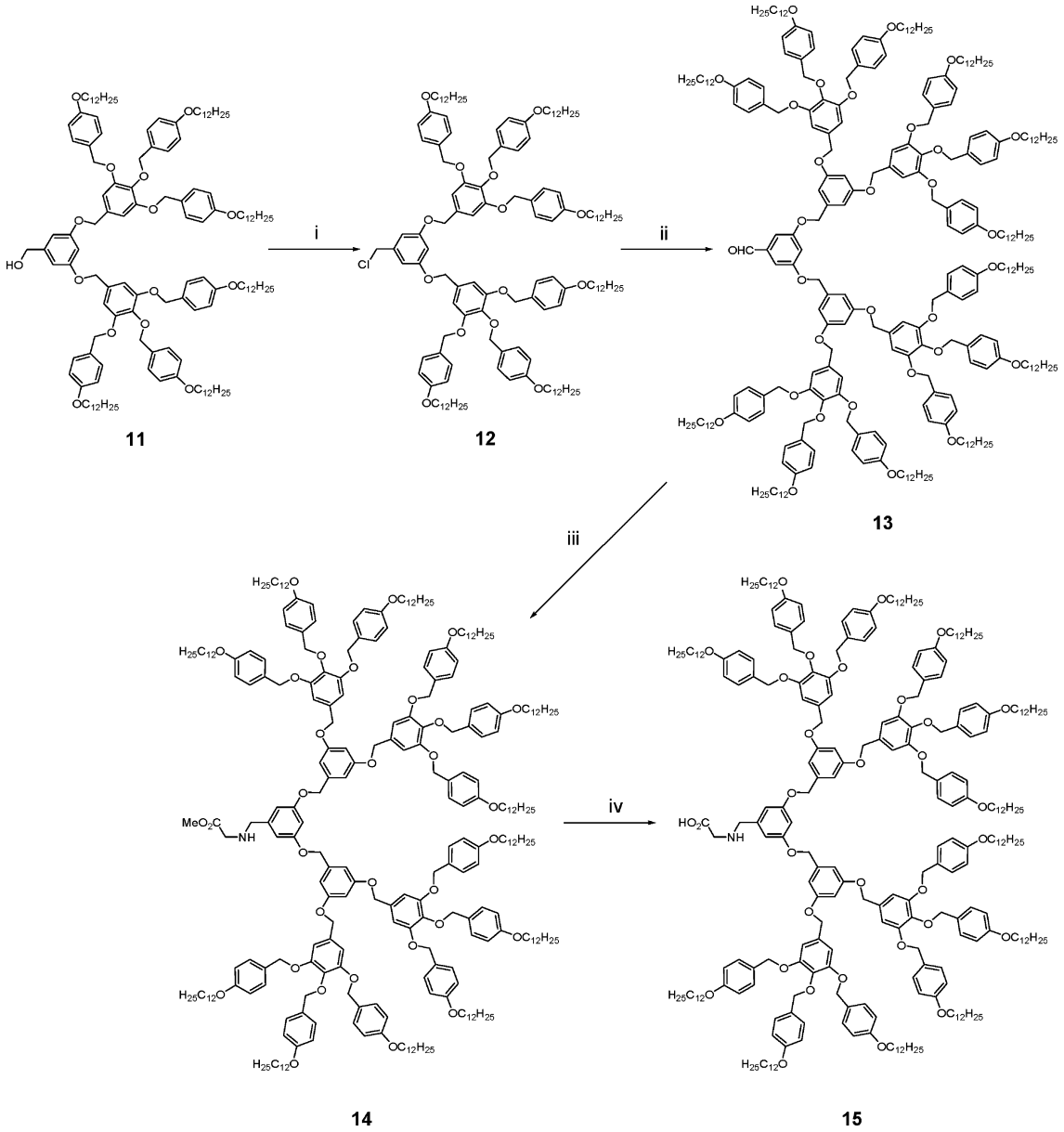

[a] (i) $SOCl_2$, 2,6-di-*tert*-butyl pyridine, CH_2Cl_2, rt, 20 min, quantitative yield; (ii) 3,5-dihydroxybenzaldehyde, K_2CO_3, DMF/THF, 80 °C, overnight, 60%; (iii) glycine methyl ester hydrochloride, Et_3N, THF/MeOH, rt, 1 h, then $NaBH_3CN$, overnight, 72%; (iv) NaOH 4 N, THF/MeOH, rt, 45 min, 95%.

to 10.1 kDa) and their a priori noncylindrical molecular shape, the sharpness and the high number of X-ray reflections indicate that the dendrimers produce well-developed smectic phases with thin interfaces between the layers, that is, highly microsegregated mesostructures (in agreement with conclusions derived from the solution properties described below). Such microsegregated structures have been observed for liquid−crystalline dendrimers such as poly(propylene imine)s, poly(amido amine)s, and poly(carbosilane)s functionalized at their periphery with calamitic mesogens.[20] These dendrimers display smectic phases in which the dendritic core (which can be strongly deformed) occupies a central sublayer and the mesogenic units are located parallel to one another, extending up and down from the dendritic core. Compounds **4**−**6** may appear different because of their more rigid C_{60} core and to the polar nature of the dendrimer, since the mesogenic cyanobiphenyl groups are attached to only one side of the molecule. Therefore, the smectic layers are likely stabilized by strong lateral and dipolar interactions between the cyanobiphenyl mesogenic groups, through the antiparallel arrangement of the fullerodendrimers forming one central sublayer, and the poly(benzyl ether) dendrons being ejected to another sublayer (see below for a detailed description of the supramolecular organization). Such an intramolecular segregation occurs above the glass transition, giving enough flexibility to the poly(benzyl ether) dendron and the aliphatic spacers of the poly(aryl ester) dendron to deform in order to favor parallel arrangement of the mesogenic groups, thus producing well-developed lamellar structures.

The second observation concerns the values of the layer spacing, which increases only slightly with increasing molecular weight, and molecular areas. To understand the molecular organization within the layers, the molecular areas were calculated from the estimated molecular volumes and layer

(20) Donnio, B.; Guillon, D. *Adv. Polym. Sci.* **2006**, *201*, 45.

Scheme 3 [a]

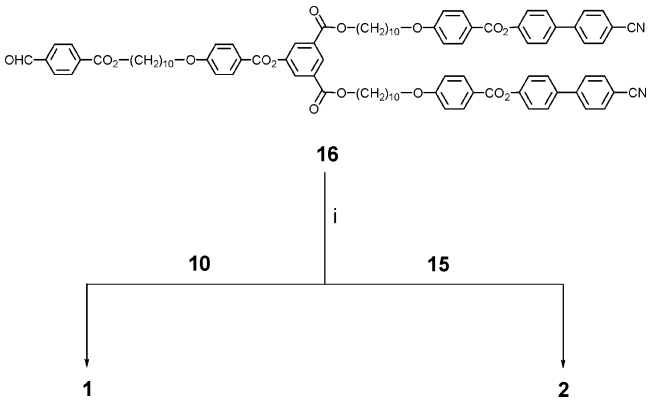

[a] (i) [60]Fullerene, toluene, reflux, overnight; yield: for **1**, 52%; for **2**, 51%.

Scheme 4 [a]

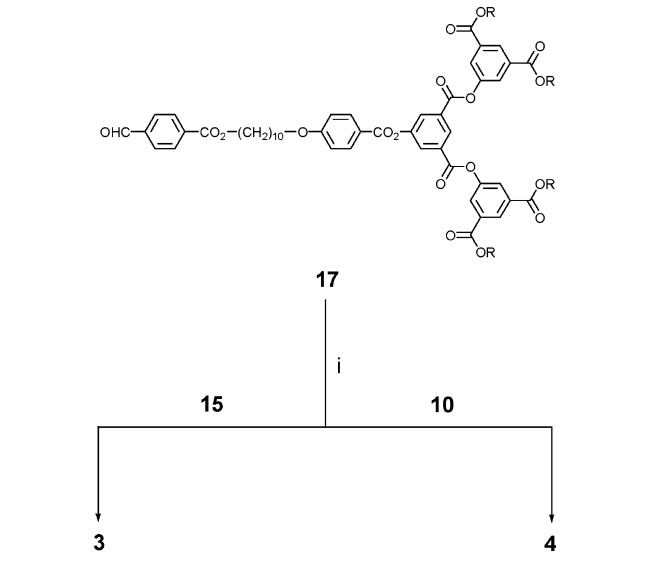

[a] (i) [60]Fullerene, toluene, reflux, overnight; yield: for **3**, 49%; for **4**, 70%. For R, see Chart 2.

thicknesses. A bilayered structure (molecules arranged head-to-head) is envisaged, where the central slab of the layer is made up of the cyanobiphenyl mesogenic groups arranged in an antiparallel fashion and the aliphatic chains of the poly(benzyl ether) dendrons pointing out at both interfaces of the layer as assumed above. In this model, the area available for each aliphatic chain is, for example, for **4**, $a_{ch} = 24-27$ Å^2 and that for each cyanobiphenyl mesogenic group $a_{mes} = 37-40$ Å^2. The former value is compatible with that found in smectic liquid crystals for disordered aliphatic chains oriented, on average, normal to the smectic layers; the latter value is compatible for mesogenic units tilted with respect to the normal of the layer. This molecular arrangement is directly related to the number of aliphatic chains (six) and mesogenic groups (four) within one molecule of **4**, knowing that the cross section of both moieties is roughly the same (about 22−25 Å^2). For **5**, one molecule contains six aliphatic chains and eight mesogenic groups. Thus, the area available for each aliphatic chain is $a_{ch} = 34-39$ Å^2 and that for each cyanobiphenyl mesogenic unit is $a_{mes} = 26-29$ Å^2. This implies that the aliphatic chains are, on average, more spread out to compensate for the increase in molecular area and that the mesogenic groups are lying normal to the layer. For **6**, the ratio of aliphatic chains to the number

Scheme 5 [a]

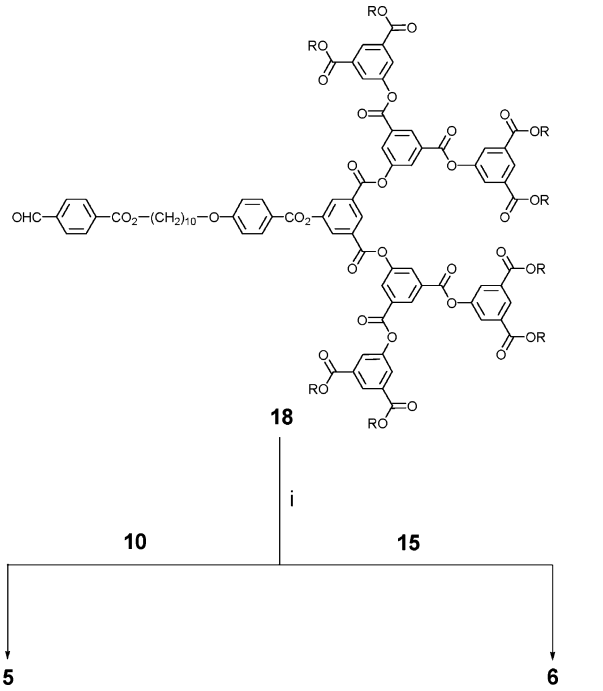

[a] (i) [60]Fullerene, toluene, reflux, overnight; for **5**, 68%; for **6**, 50%. For R, see Chart 2.

Table 1. Phase Transition Temperatures[a] and Enthalpies of Compounds **8**, **9**, **13**, and **14**, Fullerodendrimers **1**−**6**, and Model Compounds **MC-I** and **MC-II**

compd	T_g (°C)	transition	temp (°C)	ΔH (kJ·mol^{-1})	ΔH (kJ·mol^{-1}) per cyanobiphenyl unit
8	*b*	Col → I	90	6.0	
9	*b*	Col → Cub	58	2.4	
		Cub → I	74	2.2	
13	49	Col → I	105	6.0	
14	39[c]	Col → I	107	8.4	
1	31	Col$_r$-*c2mm* → I′	105[d]		
		I′ → I	108[d]	13.9[e]	7.0
2	*b*	Col$_r$-*p2gg* → I	109	16.4	8.2
3	*b*	Col$_r$-*c2mm* → I	152	23.7	5.9
4	*b*	SmC → SmA	116[f]		
		SmA → I	155	21.7	5.4
5	*b*	SmA → I	210	46.5	5.8
6		G → SmA	139	6.7	0.8
		SmA → I	209	34.7	4.3
MC-I	31	G → SmA	141	13.0	1.6
		SmA → I	209	41.4	5.2
MC-II	23	G → Col$_r$-*c2mm*	84	2.4	1.2
		Col$_r$-*c2mm* → I	105	16.9	8.5

[a] G = amorphous solid, T_g = glass transition temperature, SmC = smectic C phase, SmA = smectic A phase, Col = columnar phase, Col$_r$-*c2mm* = rectangular columnar phase of *c2mm* symmetry, Col$_r$-*p2gg* = rectangular columnar phase of *p2gg* symmetry, Cub = cubic phase, I and I′ = isotropic liquids. Temperatures are given as the onset of peaks obtained during the second heating run (rate: 10 °C min^{-1} if not stated otherwise). T_g values are determined during the first cooling run. [b] Not detected. [c] Determined during the second heating run. [d] Rate: 5 °C min^{-1}. [e] Sum of enthalpies. [f] Determined by polarized optical microscopy.

of mesogenic groups is the same (1.5) as that for **4**, leading to similar values for the corresponding areas available for the chains ($a_{ch} = 22-23$ Å^2) and cyanobiphenyl mesogenic groups ($a_{mes} = 33-34$ Å^2), and thus to a similar molecular organization.

In summary, the supramolecular organization of **4**−**6** is governed by (1) the "aliphatic terminal chains/mesogenic groups" ratio, *R*, (2) effective intra- and intermolecular lateral interactions between the cyanobiphenyl mesogenic groups, (3)

Table 2. X-ray Characterization of the Mesophases: Indexation of the Smectic Phases of Fulleropyrrolidines **4**−**6** and Characteristic Parameters of the Mesophases[a]

compd	*T* (°C)	d_{00l}(meas) (Å)	d_{00l}(theor) (Å)	parameters
4	100	$d_{001} = 121.5$	$d_{001} = 120.8$	$V_M = 9102$ Å^3
		$d_{002} = 60.4$	$d_{002} = 60.4$	$A_M = 150.7$ Å^2
		$d_{003} = 40.2$	$d_{003} = 40.25$	$a_{ch} = 25.1$ Å^2
		$d_{004} = 30.1$	$d_{004} = 30.2$	$a_{mes} = 37.7$ Å^2
5	100	$d_{001} = 125.9$	$d_{001} = 125.8$	$V_M = 13434$ Å^3
		$d_{002} = 62.95$	$d_{002} = 62.9$	$A_M = 213.6$ Å^2
		$d_{003} = 41.9$	$d_{003} = 41.95$	$a_{ch} = 35.6$ Å^2
				$a_{mes} = 26.7$ Å^2
6	150	$d_{001} = 136.0$	$d_{001} = 135.7$	$V_M = 17819$ Å^3
		$d_{002} = 68.0$	$d_{002} = 67.85$	$A_M = 262.6$ Å^2
		$d_{003} = 45.25$	$d_{003} = 45.25$	$a_{ch} = 21.9$ Å^2
		$d_{004} = 33.8$	$d_{004} = 33.9$	$a_{mes} = 32.8$ Å^2
		$d_{005} = 27.15$	$d_{005} = 27.15$	
		$d_{006} = 22.6$	$d_{006} = 22.6$	

[a] d_{00l}(meas) and d_{00l}(theor) are the measured and theoretical diffraction spacings; d_{00l}(theor) is deduced from the following mathematical expression: $<d> = 1/N_l \times \sum(l \cdot d_{00l})$; l is the miller index, N_l is the number of reflexions, *00l* are the indexations of the reflections corresponding to the smectic phases, and d is the periodicity, A_M is the molecular area ($A_M = 2V_M/d$), and a_{ch} and a_{mes} are the cross section of one chain of the dendrimer and of one cyanobiphenyl group, respectively. The molecular volume was calculated from the equation $V_M = V_{C60} + M_{dend}/(d \times 0.6022)$, where $d = V_{CH2}(T_0)/V_{CH2}(T)$, M_{dend} is the molecular weight of the dendritic part, $V_{CH2}(T) = 26.5616 + 0.02023T$ (T in °C, $T_0 = 25$ °C), the volume of a methylene group, and V_{C60} is the volume of C_{60} (700 Å^3).

effective segregation of the dendrons, and (4) the deformation of the dendritic parts to favor parallel arrangement of the cyanobiphenyl mesogenic groups. In the center of the layer, the mesogenic groups are either tilted or normal to the smectic plane, depending on *R*. In these layers, the C_{60} units are confined within well-defined sublayers, located on both sides of the central layer formed by the cyanobiphenyl groups; the poly(benzyl ether) dendritic portion is confined within external sublayers. The absence of X-ray signals corresponding to the C_{60} units suggests the absence of long-range organization and a random disposition within the sublayers. This arrangement was confirmed by molecular dynamics calculations. A periodic molecular model was created for **4** from the experimental X-ray data consisting of a quadratic cell ($250 \times 24.6 \times 24.6$ Å^3) containing eight molecules arranged in a head-to-head orientation. This structure was first minimized, and then a molecular dynamics study was performed at 373 K for 80 ps. The result of the calculations evidenced a good filling of the available volume, and the enhancement of the microsegregation was observed over the entire simulation experiment time, contributing to the stabilization of the smectic phases. The supramolecular organization of **4** within the smectic A phase is shown in Figure 1.

Let us consider now the case of model compound **MC-I**, which is the fullerene-free analogue of **5**. Above 141 °C, **MC-I** gave rise to a smectic A phase, which was identified by POM (focal conic and hometropic textures). Small-angle XRD experiments carried out at 160 and 180 °C displayed three fine and sharp reflections in the 1:2:3 ratio indicative of a layered structure, with a periodicity of $d = 111.5$ Å (Table S2). In the wide-angle part, a broad and intense halo corresponding to the molten chains was also detected. The mesophase can thus be assigned as a classical smectic A phase, which results from the segregation of the two dendritic parts similarly to the organization of **4**−**6**. In addition, a mid-angle diffraction signal, corresponding to a periodicity of $d = 24.0$ Å, is observed in the X-ray pattern, which is likely indicative of a short-range correlation in the direction perpendicular to the layer normal. Such a fluctuation may arise from strong steric constraints imposed by the bulky poly(benzyl ether) dendron, which periodically disrupts the ideal lateral packing and forces the various sub-blocks to be slightly shifted along the layer normal to form an "egg-box" structure. Such periodic blocks would contain ca. 3 molecules. Here, it is interesting to remark that compounds **5** and **MC-I** present a smectic A structure with a similar layer spacing ($d = 125.8$ and 111.5 Å for **5** and **MC-I**, respectively). This indicates that the driving force to establish the lamellar structure is governed by a rather similar size of the two dendritic parts (in other words, a small *R* value), the C_{60} unit playing no significant role in the supramolecular organization.

Columnar Phases. From room temperature up to about 60 °C, the X-ray patterns of **1** are characterized by diffuse signals, indicative of an amorphous state with no specific organization. Above this temperature, a rectangular columnar phase of *c*2*mm* symmetry emerges. This phase, which was identified by the high number of reflections (Table 3 and Figure S10), remains unchanged up to 105 °C, where it transforms into a viscous, isotropic phase. However, the X-ray patterns recorded in this temperature range showed no specific sharp signals, which would have indicated the formation of a cubic phase. This phase can be described as the isotropic liquid I′ similar to that observed by Goodby et al. in systems showing twisted grain boundary phases or by Kutsumizu et al. in systems showing a cubic phase.[18]

From room temperature up to 75 °C, **2** is amorphous. Above this temperature, a structure emerges evidenced by the presence of two diffuse signals at 100 and 41 Å. At yet higher temperatures, the number of sharp diffraction signals increases significantly, which allows the identification of the mesophase as a noncentered rectangular columnar phase of *p*2*gg* symmetry (Table 3 and Figure S10).

The X-ray patterns of **3** revealed two transitions, a first one at about 70 °C, which corresponds to a transition from an amorphous solid to a mesophase, and the second one at about 150 °C, which corresponds to the transition from the mesophase to the isotropic liquid. However, it should be noted that the mesophase formation kinetics are very slow; at 100 °C, the X-ray signals are wide, and it is only at 120 °C that the mesophase becomes well organized and identified by a large number of sharp diffraction peaks as a rectangular columnar phase of *c*2*mm* symmetry (Table 3 and Figure S10).

As for the first series (i.e., compounds **4**−**6**), the supramolecular organizations of **1**−**3** extend over long distances as evidenced by the presence of the large number of sharp, intense small-angle X-ray diffraction peaks. This long-range columnar ordering occurs despite the high molecular weight of the compounds (4.3−7.7 kDa) and in the absence of any molecular shape specificity that could lead to the formation of quasi-discs. In addition, it develops only above certain temperatures in such a way that the conformation of the aliphatic spacers and the dendritic moieties can adapt to the most stable condensed phase. Another feature of interest within this series is the value of the ratio *R*, which is 3 for **1** and **3**, and 6 for **2**. These values are larger than those of **4**−**6** (0.75−1.5), which exhibit smectic

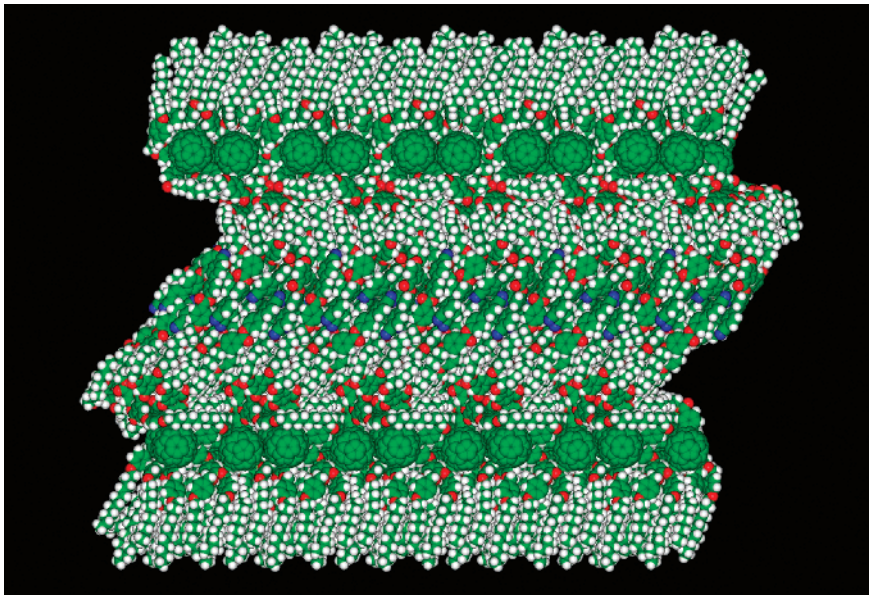

Figure 1. Postulated supramolecular organization of **4** obtained by molecular dynamics. Compounds **5** and **6** gave similar results.

Table 3. X-ray Characterization of the Mesophases: Indexation of the Columnar Phases of Fulleropyrrolidines **1**−**3** and Characteristic Parameters of the Mesophases at Representative Temperatures[a]

compd	T (°C)	d_{hk}(meas) (Å)	d_{hk}(theor) (Å)	parameters
1	75	$d_{20} = 107.6$	$d_{20} = 107.6$	Col_r-*c*2*mm*
		$d_{11} = 81.75$	$d_{11} = 81.75$	$a = 215.2$ Å
		$d_{31} = 55.8$	$d_{31} = 55.7$	$b = 88.35$ Å
		$d_{40} = 53.7$	$d_{40} = 53.8$	$S = 9506$ Å^2
		$d_{02} = 44.1$	$d_{02} = 44.2$	$V_M = 6825$ Å^3
		$d_{51} = 38.7$	$d_{51} = 38.7$	$N = 14$
		$d_{60} = 35.75$	$d_{60} = 35.9$	
		$d_{42} = 34.0$	$d_{42} = 34.15$	
2	90	$d_{20} = d_{11} = 98.6$	$d_{20} = d_{11} = 98.6$	Col_r-*p*2*gg*
		$d_{21} = 74.0$	$d_{21} = 74.5$	$a = 197.2$ Å
		$d_{31} = d_{02} = 56.5$	$d_{31} = d_{02} = 56.9$	$b = 113.85$ Å
		$d_{22} = 49.1$	$d_{22} = 49.3$	$S = 11226$ Å^2
		$d_{41} = 45.6$	$d_{41} = 45.25$	$V_M = 10665$ Å^3
		$d_{32} = 42.9$	$d_{32} = 43.0$	$N = 10$
		$d_{51} = d_{42} = d_{13} = 37.1$	$d_{51} = d_{42} = d_{13} = 37.3$	
		$d_{33} = 33.4$	$d_{33} = 32.9$	
3	120	$d_{20} = 120.1$	$d_{20} = 120.1$	Col_r-*c*2*mm*
		$d_{11} = 104.25$	$d_{11} = 104.25$	$a = 240.2$ Å
		$d_{31} = 65.4$	$d_{31} = 65.8$	$b = 115.7$ Å
		$d_{40} = 59.75$	$d_{40} = 60.0$	$S = 13896$ Å^2
		$d_{51} = 44.2$	$d_{51} = 44.4$	$V_M = 13074$ Å^3
		$d_{42} = 40.8$	$d_{42} = 41.6$	$N = 10$

[a] d_{hk}(meas) and d_{hk}(theor) are the measured and theoretical diffraction spacings; d_{hk}(theor) is deduced from the following mathematical expression: $1/d_{hk} = \sqrt{(h^2/a^2+k^2/b^2)}$; *hk* are the indexations of the reflections corresponding to the rectangular symmetry, and *a* and *b* are the lattice parameters of the Col_r phase, *S* is the columnar cross section ($S = 1/2 \cdot a \times b$). The molecular volume was calculated from the equation: $V_M = V_{C60} + M_{dend}/(d \times 0.6022)$, where $d = V_{CH2}(T_0)/V_{CH2}(T)$, M_{dend} is the molecular weight of the dendritic part, $V_{CH2}(T) = 26.5616 + 0.02023T$ (T in °C, $T_0 = 25$ °C), the volume of a methylene group, and V_{C60} is the volume of C_{60} (700 Å^3). *N* is the number of molecular equivalents per slice of column 10 Å thick.

phases, and are consistent with an induced curvature in the structure, leading to columnar phases, as, for example, with polycatenar liquid crystals.[21]

To understand the supramolecular organization of **1**−**3** in the columnar phases, the number of molecules per unit length along the columnar axis was calculated from the rectangular lattice parameters and the estimated molecular volumes (Table 3). A columnar slice of 10 Å thickness (corresponding roughly to the diameter of C_{60}) contains 14 molecules of **1** and 10 molecules of the larger dendrimers **2** and **3**. The postulated model of the molecular organization (Figure 2) is derived from that of the lamellar organization of **4**−**6**. Since the number of aliphatic chains in **1**−**3** is larger than the number of cyanobiphenyl mesogenic groups, the transverse molecular areas of both molecular moieties are significantly different, and therefore a stable lamellar structure cannot be obtained. Increasing *R* destabilizes the layering by breaking the layers into ribbons as previously observed for the lamellar-to-columnar phase transition exhibited by biforked liquid crystals,[22] carbosilane dendrimers of fifth generation,[23] and statistical liquid−crystalline

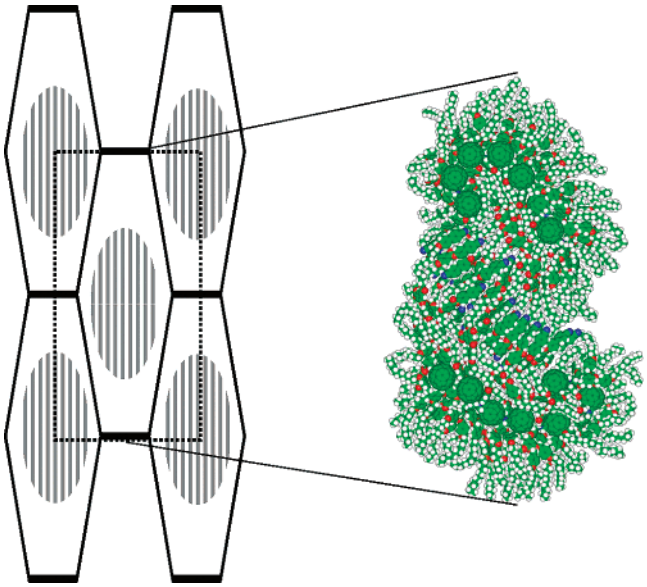

Figure 2. Postulated supramolecular organization of **1** within the rectangular columnar phase of *c*2*mm* symmetry. Compounds **2** (Col_r-*p*2*gg*) and **3** (Col_r-*c*2*mm*) gave a similar organization. For the symmetry of the Col_r-*p*2*gg* phase, see Figure S11.

(21) Nguyen, H. T.; Destrade, C.; Malthête, J. *Adv. Mater.* **1997**, *9*, 375.

(22) Guillon, D.; Heinrich, B.; Ribeiro, A. C.; Cruz, C.; Nguyen, H. T. *Mol. Cryst. Liq. Cryst.* **1998**, *317*, 51.

codendrimers.[24] Intrinsically, each columnar core is made up of mesogenic groups interacting through the cyanobiphenyl groups and is surrounded by the poly(benzyl ether) dendrons including the C_{60} units.

Thus, as for compounds **4**−**6**, the supramolecular organizations of **1**−**3** are also governed by the ratio *R*, the microsegregation, the core deformation, and the specific interactions between the cyanobiphenyl groups. A competition occurs between the tendency of the cyanobiphenyl subunits to form layers via a head-to-head arrangement and the bulky dendrons forcing a columnar arrangement. This competition is dominated by the bulky dendrons evidenced by the presence of strong layer undulations with large amplitudes which result in the destruction of the layers into ribbons. For $R = 3$, the average columnar cross section resembles that of a bow tie, and the optimal organization is a centered lattice (i.e., for **1** and **3**). However, as *R* increases, the cross section becomes more circular (large dendrons), generating a noncentered lattice (i.e., for **2**).

Within the supramolecular organizations, molecular aggregates are formed and arranged into columns. Strong microsegregation between incompatible regions results in each constitutive part being confined to a specific region: the cyanobiphenyl subunits form the columnar center and the dendrons form the surrounding crown. The C_{60} units are localized at the interface along the *b*-direction (the shortest one). The absence of X-ray signal corresponding to C_{60} suggests a loose disposition of the latter.

This arrangement was confirmed by molecular dynamics calculations on **1**. A periodic molecular model was created from the XRD data and consisted of a nearly quadratic cell ($210 \times 200 \times 10$ Å^3), where 10 Å correspond to the thickness of one virtual slice and the C_{60} diameter: 14 molecules were placed in a head-to-head fashion, and the structure was first minimized. A molecular dynamics study was then performed at 348 K for 80 ps. The result of the calculations evidenced good filling of the available volume, and enhancement of the microsegregation was observed over the entire simulation time, contributing to the stabilization of the columnar phases.

It is of interest to consider now model compound **MC-II**, which is the fullerene-free analogue of **1**. **MC-II** gave rise to a rectangular columnar phase of *c*2*mm* symmetry between 84 and 105 °C, with lattice parameters $a = 237.8$ Å and $b = 77.75$ Å (Table S4). Moreover, an additional short-range periodicity was measured in the *c*-direction, indicative of some columnar fluctuations or undulations. This periodicity of about 26.5 Å would correspond to the length of a columnar bundle (about 40 molecules) of a periodically pinched column. Thus, **1** and **MC-II** exhibit the same columnar structure with similar lattice parameters. This indicates that the supramolecular organization is, once more, imposed by the dendritic parts, the size of which is very different (in other words, a high *R* value), whatever the presence or not of the C_{60} unit.

In summary, the model compounds and their fullerene analogues gave rise to similar mesomorphism (nature of mesophases and clearing points). This result indicates that, in **1**−**6**, the C_{60} unit does not dictate the overall molecular shape as for homodendrimers also based on poly(benzyl ether) dendrons.[25] In the latter case, the presence of C_{60} led to spherical structures, which did not display mesomorphism. The beneficial effect of codendritic architectures to generate mesomorphism for fullerodendrimers is therefore clearly demonstrated by **1**−**6**.

Solution Properties. To estimate the effect of each dendron on the molecular properties of the fullerodendrimers, the solution properties of **3**, **13**, and **17** (Table 4) were examined in benzene. The permanent dipole moments (μ) of **3**, **13**, and **17** were measured by the Guggenheim−Smith method.[26] This method is derived from the experimental determination of the dielectric permittivity increment $(\epsilon - \epsilon_o)/c$, where $(\epsilon - \epsilon_o)$ is the difference between the dielectric permittivity of the solution and solvent, and on the determination of the squared refractive index increment $(n^2 - n_o^2)/c$, where n and n_o are the refractive indices of the solution and solvent, respectively, and c is the solute concentration. The dipole moments (μ) were calculated according to eq 1.[27]

$$\mu^2/M = 27kT[(\epsilon - \epsilon_o)/c - (n^2 - n_o^2)/c]/[4\pi N_A(\epsilon_o^2 + 2)^2] \quad (1)$$

Linear concentration dependencies of $(\epsilon - \epsilon_o)$ (Figure S12) and $(n^2 - n_o^2)$ (Figure S13) were observed. The increments $(\epsilon - \epsilon_o)/c$ and $(n^2 - n_o^2)/c$ were determined from the gradients and are reported in Table 4.

Table 4. Molecular Weight (M), Hydrodynamic Diameter (d_h), Permanent Dipole Moment (μ), Molar Kerr Constant (K_M), Dielectric Permittivity Increment $[(\epsilon - \epsilon_o)/c]$, and Squared Refractive Index Increment $[(n^2 - n_o^2)/c]$ of **3**, **13**, and **17**

compd	M (Da)	d_h (Å)	μ (D)	$K_M 10^8$ (cm^5 (300 V)$^{-2}$ mol^{-1})	$(\epsilon - \epsilon_o)/c$ (cm^3 g^{-1})	$(n^2 - n_o^2)/c$ (cm^3 g^{-1})
3	7679	45 ± 5	19.2 ± 0.8	5.5 ± 0.3	6.2 ± 0.2	0.13 ± 0.01
13	4228	33 ± 5	6.4 ± 0.5	0.4 ± 0.1	1.3 ± 0.1	0.09 ± 0.01
17	2733	34 ± 4	14.2 ± 0.9	4.5 ± 0.3	9.4 ± 0.3	0.10 ± 0.01

Electrooptical molar Kerr constants (K_M) of **3**, **13**, and **17** were obtained according to eq 2.[28]

$$K_M = \frac{6n_0M}{(n_0^2 + 2)^2(\epsilon_0 + 2)^2}\left(\frac{\Delta n - \Delta n_0}{E^2 c}\right)_{c\to 0} \quad (2)$$

The variation of optical birefringence (Δn) as a function of E^2 was determined for different concentrations of **17** (Figure S14). No deviation from Kerr law (according to which, optical birefringence (Δn) increases linearly with E^2 in molecular dispersed liquids) was observed. Similar results were obtained for **3** and **13**.

From the variation of $(\Delta n - \Delta n_0/E^2c)$ as a function of concentration (Figure S15), the $(\Delta n - \Delta n_0/E^2c)_{c\to 0}$ values were obtained at $c = 0$ for **3**, **13**, and **17** and used for the calculation of K_M according to eq 2.

(23) Richardson, R. M.; Ponomarenko, S. A.; Boiko, N. I.; Shibaev, V. P. *Liq. Cryst.* **1999**, *26*, 101.
(24) Rueff, J.-M.; Barberá, J.; Donnio, B.; Guillon, D.; Marcos, M.; Serrano, J.-L. *Macromolecules* **2003**, *36*, 8368.
(25) Scanu, D.; Yevlampieva, N. P.; Deschenaux, R. *Macromolecules* **2007**, *40*, 1133.
(26) Oehme, F. *Dielektrische Messmethoden zur quantitativen Analyse und für Chemische Strukturbestimmungen;* Verlag Chemie: Weinheim, Germany, 1962.
(27) N_A, Avogadro's number; *M*, molecular mass of the solute; *k*, Boltzmann constant; *T*, temperature in Kelvin.
(28) $\Delta n - \Delta n_o$, difference between the optical birefringence of the solution (solute of concentration *c*) and solvent, respectively; *E*, strength of the electric field. The value $(\Delta n - \Delta n_o/E^2c)_{c\to o}$ is determined for an infinite dilution.

The hydrodynamic molecular diameters d_h (Table 4) were calculated using the molecular translation diffusion coefficients D measured in benzene at 25 °C.[29] These calculations are based on the spherical model of molecules according to the Stokes−Einstein eq 3.[30]

$$d_h = kT/3\pi\eta_o D \quad (3)$$

The data reported in Table 4 indicate that the permanent dipole moment (μ) and Kerr constant (K_M) values of **13** (carrying aliphatic chains) and **17** (carrying cyanobiphenyl groups) are in agreement with their structure and polarity.

Knowing that molar Kerr constants (K_M) are additive in solution, when the elecrooptical properties of specific fragments of a molecule are known, it is possible to verify the degree of freedom of those fragments within the molecule.[29] The K_M value for **3** can be calculated from eq 4 using the molar Kerr constant values of **13** and **17** and their corresponding weight fractions $w_1 = 0.55$ and $w_2 = 0.36$ in **3**.

$$K_M = K_{M1}w_1 + K_{M2}w_2 \quad (4)$$

According to eq 4, the calculated K_M value for **3** is 1.9×10^{-8} cm^5 $(300\ V)^{-2}$ mol^{-1}, which is significantly smaller than the experimental value (Table 4). This result reveals that the rotational freedom of the two dendritic fragments is limited by the rigidity of the fulleropyrrolidine unit. The fact that the dipole moment value of **3** is approximately equal to the sum of the dipole moment values of both dendrons (Table 4) provides further evidence of the structural rigidity of **3**. This situation is reached because in compound **3** dendrons **13** and **17** are rigidly linked and rotate synchronically in the external electric field.

The hydrodynamic dimensions (d_h) of **13** and **17** are identical, within experimental error (Table 4), indicating that **13** is more folded than **17**. Considering the differences in molecular weight and permanent dipole moments of each dendron, the properties of **3** would indicate a nonequivalent distribution of mass and polarity, whereby the molecule is made up of a heavier part (subunit **13**) and a more polar part (subunit **17**) of similar sizes. Such a structural specificity should be responsible for the molecular packing and microsegregation discussed above.

(29) Tsvetkov, V. N. *Rigid-Chain Polymers: Hydrodynamic and Optical Properties in Solution;* Consultants Bureau: New York, 1989.
(30) η_o, viscosity of the solvent.

Conclusion

We have demonstrated that the 1,3-dipolar addition is an efficient reaction for the synthesis of fullero(codendrimers). This reaction permits the design of a great variety of functional macromolecules with sophisticated structures. In this study, a poly(benzyl ether) dendron, which displays columnar mesomorphism, was linked to a poly(aryl ester) dendron, which shows smectic mesomorphism. Depending on the respective size of each dendron, either smectic or columnar phases were obtained. Therefore, tuning of the mesomorphism for fullerene-containing liquid crystals is successfully reached *by design*. XRD investigations, molecular modeling, and solution studies revealed that the supramolecular organization of the title compounds is governed by (1) the "aliphatic terminal chains/mesogenic groups" ratio, (2) the effective lateral interactions between the cyanobiphenyl mesogenic groups, (3) the effective microsegregation of the dendrons, and (4) the deformation of the dendritic core. It is noteworthy that the supramolecular organization within the mesophases extends over long distances, evidenced by the presence of a large number of sharp and intense small-angle XRD peaks. Moreover, typical textures for the mesophases were observed by POM, textures usually found for low molar mass liquid crystals. Therefore, both XRD and POM results confirmed the high degree of organization of the fullerodendrimers within the mesophases.

Acknowledgment. R.D. thanks the Swiss National Foundation (Grant No. 200020-111681) for financial support. We thank Dr. C. Bourgogne for molecular dynamics studies and Dr. I. Zaitseva for the determination of the diffusion coefficient. B.D. and D.G. thank CNRS and ULP for financial support.

Supporting Information Available: Techniques, instruments, synthetic procedures, and analytical data of all new compounds. This material is available free of charge via the Internet at http://pubs.acs.org.

JA071012O